2-1-2 Solar Energetic Particle Prediction and Alert

KUBO Yûki, NAGATSUMA Tsutomu, and AKIOKA Maki

Cosmic radiation is a commonly known source of exposure to natural radiation for astronauts and artificial satellites. The phenomenon of solar energetic particles suddenly increasing in intensity is one of the most hazardous events. This paper first introduces statistical and simulation approaches to predicting and alerting the occurrence of solar energetic particles. It then reviews the development of a space environment reporting system designed to detect solar energetic particles in the early stages of occurrence and disseminate related information.

Keywords
Solar energetic particles, Particles transport, Radiation hazard, Event reporting system

1 Introduction

Now as the sphere of human activity is expanding into space, space environmental disturbances more often than not threaten the security and safety of human life. Given this situation, the technique for space weather forecasting to gain a precise insight into space environmental disturbances, as well as to predict them and issue alerts, is assuming greater importance. In particular, as space travel becomes a reality, such as the International Space Station (ISS) manned by astronauts for extended periods of time orbiting in space, possible exposure to cosmic radiation poses a very serious challenge to the health of astronauts and other crew members.

The term "cosmic radiation" refers to the ionizing radiation present in space and can be broadly divided into three types according to the origin: galactic cosmic rays, solar energetic particles, and radiation belt particles. From the standpoint of astronauts being exposed to radiation hazards, galactic cosmic rays and solar energetic particles are important. Galactic cosmic rays arriving from outside the solar system are generally believed to have constant intensity on a short time scale compared to the solar activity cycle of 11 years, with the radiation dose aboard ISS being estimated at about 0.5 mSv a day. This is roughly comparable to the radiation dose experienced in a chest CT scan test once every two weeks. In contrast, solar energetic particles subject to sudden increases in intensity under the influence of solar flares or similar events are estimated to result in a radiation dose a dozen to several tens of times higher than normal[1]. This suggests that avoiding exposure to solar energetic particles is necessary for protection against radiation hazards. Astronauts on an extended period of stay aboard the ISS or traveling to the Moon, Mars or elsewhere onboard manned spacecraft should therefore benefit from being alerted to the occurrence of solar energetic particles, and thus notified of the risks of solar energetic particles.

There are two broad conceptual approaches to issuing alerts on the occurrence of solar energetic particles. One involves alerts regarding occurrence of the events themselves. The other involves alerts on time variations in the solar energetic particle flux. Figure 1 shows an example of extremely large solar energetic particle flux observed immediately after the events initially occurred. In this case, issuing an alert on occurrence of the events them-

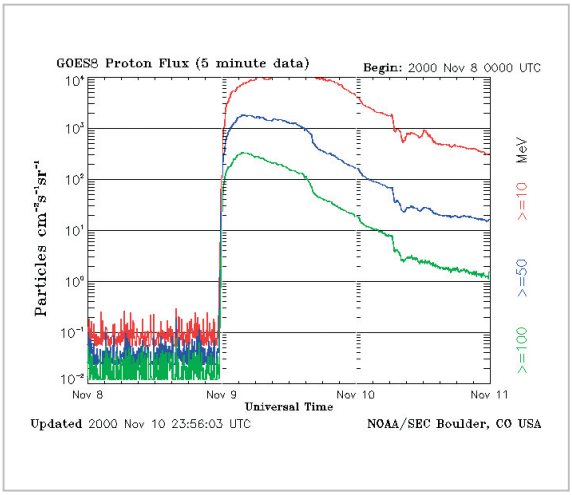

Fig. 1 *Solar energetic particle events (reprinted from Space Weather Prediction Center, NOAA Website)*

selves is very important. Since the present state of the art does not yet allow us to identify the mechanism of particle acceleration or comprehend the physics of solar flares and CMEs (coronal mass ejections) involved with the particle acceleration, the work of predicting the occurrence of the events with physical justification is extremely difficult or impracticable to achieve. As a workaround, techniques adhering to empirical rules based on observational data have been proposed[2]-[7].

At the same time, the significance of time variations in solar energetic particle flux following occurrence of the events, particularly the peaks in particle flux and total particle flux alerts, has been pointed out[8]. This may be predictable with some physical justification given the process of solar energetic particle propagation through the solar wind, and related attempts are now underway (see[9]).

Along with these attempts, a space environment event reporting system is being developed to disseminate information about occurrence of the events in its early stages.

This paper discusses a study of alerts on the occurrence of the solar energetic particle events based on the empirical rules described in Reference[2] in Chapter **2**. Chapter **3** describes a study of predicting time variations in solar energetic particle flux by means of simulation, and Chapter **4** introduces the development of a space environment event reporting system.

2 Occurrence of the solar energetic particle events

Since the present state of the art does not yet allow us to identify the mechanism of particle acceleration or comprehend the physics of solar flares and CMEs involved with the particle acceleration, the work of predicting occurrence of the events with physical justification is impracticable to achieve. Under these circumstances, deriving empirical rules regarding occurrence of the events by analyzing observational data would provide a promising solution to alerts regarding occurrence of the solar energetic particle events.

We analyzed X-ray flare data as observed by GOES (**G**eostationary **O**perational **E**nvironment **S**atellite) to delve into the properties of X-ray flares that generate the solar energetic particle events, in an attempt to derive empirical rules regarding occurrence of the events.

2.1 Data analyses

To issue alerts on the occurrence of solar energetic particles, observational data made available in real time must be analyzed. To this end, we used soft X-ray flux and solar energetic particle intensity data as observed by the GOES satellite. The term "solar energetic particle events" lacks a strict definition since it may occur on a variety of scales. For the sake of convenience, particles having energy of at least 10 MeV, with intensity exceeding 10 protons $cm^{-2}sec^{-1}sr^{-1}$ (as observed by the GOES satellite), are defined as solar energetic particles. The ISES (**I**nternational **S**pace **E**nvironment **S**ervice) uses this definition as a standard for space weather prediction and is a requirement imposed from the perspective of engineering, not physics. Solar energetic particle events matching this definition are called "proton events." From the standpoint of space weather prediction, variations of the solar energetic particle events not meeting this defi-

nition are excluded from the scope of our discussions. The analysis period was from January 1997 to mid-July 2002.

Proton events are considered to normally occur in connection with large solar flares. Although the scale of a solar flare is generally expressed as a peak X-ray flux (such as an M1.0 class flare), the time integral of an X-ray flux (also known as "fluence"), which is considered relevant to the total energy emitted by flares, may provide a better indicator. In this work, fluence is therefore used as an indicator of solar flare scale. Fluence is defined as a time integral of an X-ray flux, and can be expressed as:

$$F_t = \int_{t_s}^{t_e} F(t) - F(t_s)dt$$

where, F_1, $F(t)$, t_s and t_e denote the fluence, X-ray flux, flare start time, and flare end time, respectively. The background level is assigned as a flux value of the X-ray flare start time. The flare start time has been identified by NOAA's **S**pace **W**eather **P**rediction **C**enter (SWPC). The flare end time is defined as the time when the X-ray flux has diminished to half of its maximum.

Fig. 2 shows the relation between the maximum proton intensity and the fluence of flares that produce proton events (proton flares). The flare (C1.7 class) at the leftmost point in the diagram can be ignored from the scope of subsequent discussions for certain reasons. As shown in Fig. 2, some relation may exist between the maximum proton intensity and the fluence of X-ray flares, but the correlation coefficient between both is only about 0.43 and inadequate to confirm a correlation. Figure 2 also shows that proton flares have a fluence value of at least 20 ergs cm^{-2}. This finding is important, because it helps us conclude that no proton events will occur as long as proton flares have a fluence value lower than 20 ergs cm^{-2}.

Fluence used as an indicator of flare scale is defined here as a time integral of flux as expressed in Equation (1), but generally the peak X-ray flux is used as described earlier.

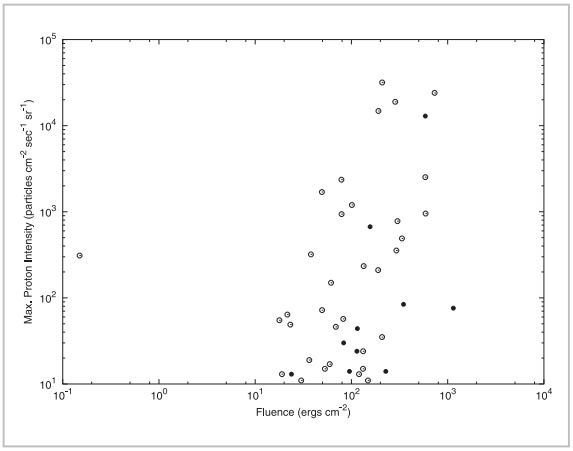

Fig.2 *Relation between maximum proton intensity and proton flare fluence*

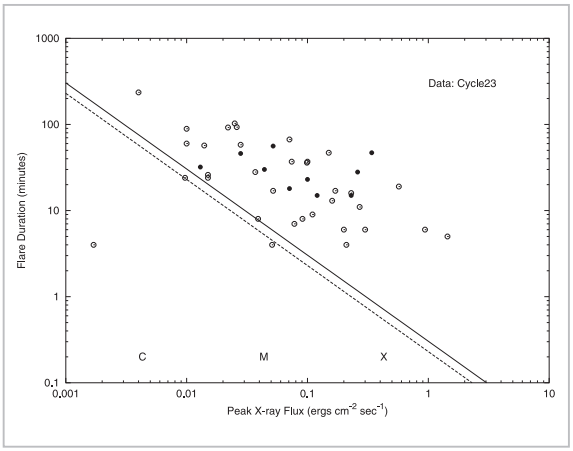

Fig.3 *Relation between peak X-ray flux of proton flares in solar cycle 23 (during the analysis period) and flare duration, and threshold line drawn by solving Equation (1)*

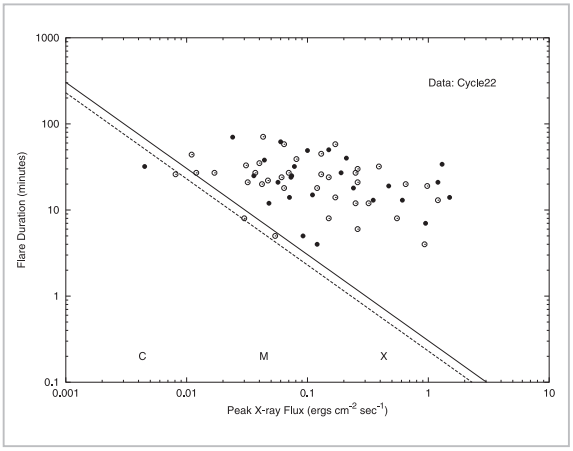

Fig.4 *Similar to Fig. 3, except that the data points are those in solar cycle 22.*

Accordingly, the results above can be made easier to understand intuitively and become more useful from a real-time alerting standpoint when expressed using the peak X-ray flux. Data analyses of the proton flares used this time draw on the existence of the following relation between fluence F_l and peak X-ray flux F_p expressed as:

$$F_p \cdot D = 1.0076\, F_t^{\,0.96633} \qquad (1)$$

where, D denotes the duration of the flare defined as $D = t^c - t^m$, and t^m the time at the peak X-ray flux. Using this equation along with the threshold of proton event occurrence F_t = 20 ergs cm^{-2}, a threshold line (D = 18.2 F_p^{-1}) can be drawn in the F_p–D plane as shown in Fig. 3.

Figures 3 and 4 plot the durations and threshold lines of proton flares in solar cycles 23 and 22, respectively, with respect to the peak X-ray flux. As can be seen from these diagrams, nearly all proton flares sit above the threshold lines, indicating the presence of thresholds during the flare duration with respect to the peak X-ray flux. For example, only M1.0 class flares having a duration of about 30 minutes or longer can produce proton events. In the past, it had been empirically stated that solar flares of the M class or higher having a longer duration are more likely to produce proton events, a statement now legitimately endorsed by data.

Figure 5 plots the fluence distributions of all C class and higher flares (observed about 10,000 times) that occurred during the analysis period. Evidently, a majority of these flares have fluence values of 20 ergs cm^{-2} or lower, and flares that could produce proton events were rare. During the analysis period, flares meeting the proton flare requirement were observed about 400 times, as compared with proton events being observed only about 60 times. This means that all flares meeting the fluence requirement of at least 20 ergs cm^{-2} did not produce proton events. From this finding, it is concluded flares failing to meet the fluence requirement of at least 20 ergs cm^{-2} will not produce proton events, but one should also remember that this fluence requirement is only a necessary condition for a proton event to occur.

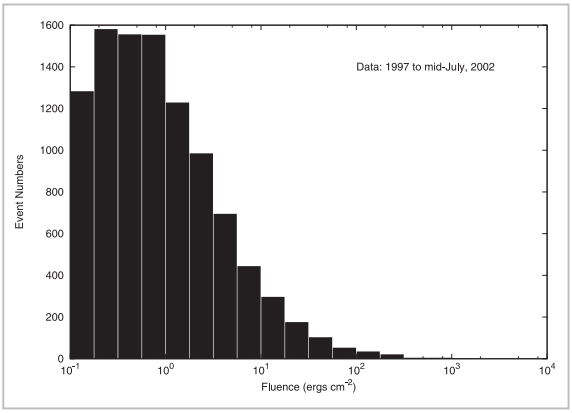

Fig.5 *Fluence distributions of all C class and higher flares occurring during the analysis period*

Yet, knowing in advance whether proton events will occur can be very useful information in making decisions on whether to call off extravehicular activities by astronauts aboard a space shuttle, ISS or other spacecraft.

3 Time variations in solar energetic particle flux

Solar energetic particles are accelerated by both the solar flare region and interplanetary shock waves. Both factors must generally be taken into account to predict time variations in the particle flux near the earth. While solar energetic particles having energy of at least 100 MeV are observed in the initial phase of a proton event, the acceleration of particles to a high energy by interplanetary shock waves is difficult to achieve. Rather, such solar energetic particles have presumably propagated through the solar wind upon being accelerated in a solar flare region or solar corona. Hence, particles accelerated by interplanetary shock waves may be set aside from the process of predicting time variations in such solar energetic particle flux. Therefore, only the propagation process of solar energetic particles accelerated near the sun through the solar wind need be heeded in considering the initial

phase of a proton event.

Solar energetic particles emitted near the sun arrive near the earth propagating through the solar wind magnetic field. Because the Larmor radius of solar energetic particles is sufficiently small compared to the global structure of the solar wind magnetic field, particles approaching the earth are aligned with magnetic field lines in the solar wind. In the meantime, small-scale magnetic field disturbances (turbulent magnetic fields) exist throughout the solar wind, thereby diffusing the solar energetic particles propagating through the solar wind. Consequently, the solar energetic particles propagate along a global magnetic field upon being diffused in the solar wind. Such a form of propagation has generally been approached numerically in a solving the Fokker-Planck equation or through simulation[9] based on a stochastic differential equation. Implementing such numeric simulations essentially requires that the diffusion coefficient tensor that provides a diffusion coefficient and drift motion, and a pitch angle diffusion coefficient relevant to the mean free path be defined in a quantitative manner. Although these coefficients are generally assigned analytically under various conditions of approximation, they are not necessarily valid and may deviate by a wide margin from the values evaluated by observations under varied solar wind conditions[10]. Despite those drawbacks, the calculation techniques described above are still being used since they eliminate the need to track down the motion of particles, save calculation time, and thus eliminate the need to employ supercomputers and high-speed parallel computing technique.

Recent advances in supercomputers and high-speed parallel computing technique have made high-speed computing possible. The use of such high-speed computing technique in directly tracking down the motion of solar energetic particles in a turbulent magnetic field would allow the process of particle propagation involving the diffusion process in solar wind to be reproduced[11]. Because this technique directly tracks down the motion of particles by solving an equation of motion, it eliminates the need to define a diffusion coefficient tensor or other geometric entity that describes diffusion or drift motion, thereby offering the advantage of simulating the process of solar energetic particle propagation given a degree of magnetic field turbulence. Subsequent discussions introduce a method of simulating the process of solar energetic particle propagation through the solar wind based on this technique.

3.1 Simulation of diffusion process

Three-dimensional isotropic turbulent magnetic fields are generally expressed as a superposition of numerous waves. Each wave is expressed as a trigonometric function determined by four random numbers—two in the wavenumber vector direction and one each for the polarization and phase of the wave. The turbulent magnetic field generated as a superposition of these waves may be added to background magnetic field B_0 to determine a general magnetic field as follows:

$$\vec{B} = \vec{B}_0 + \delta\vec{B}$$

$$\delta\vec{B} = \sum_{n=1}^{N} \vec{b}_n A(k_n) \exp\left[i(\vec{k}_n \cdot \vec{r} + \phi_n)\right]$$

$$A(k_n)^2 = \left(\frac{\delta B}{B_0}\right)^2 G(k_n) \left[\sum_{n=1}^{N} G(k_n)\right]^{-1}$$

$$G(k_n) = \frac{4\pi k_n{}^2 \Delta k_n}{1 + (k_n L_c)^{\gamma}}$$

γ is set to 11/3 to make $G(k_n)$ Kolmogorov-type turbulence spectrum where kn is large. L_c denotes the correlation length of the turbulence, and $\vec{b}_n$ the unit vector in the sinusoidal wave direction. Setting $\vec{k}_n \cdot \vec{b}_n = 0$ ensures that div $\mathrm{div}\vec{B} = 0$. The intensity of the turbulence can be varied by changing the value of parameter ($\delta B/Bo$). Solving the equation of motion of solar energetic particles in the resultant magnetic field will track down the motion of particles and reproduce their process of diffusion.

The first step is to perform a test calcula-

tion assuming a uniform background magnetic field to verify that the diffusion process is reproduced. Figure 6 plots the results of tracking down the motion of 10-MeV particles in a magnetic field having a turbulence intensity of 0.1. The tracks of eight sample particles are pictured in the diagram, though the simulation traced the tracks of 20,000 particles. The background magnetic field is oriented perpendicularly to the space from the opposite side of that space, suggesting that the particles have traversed the background magnetic field lines. To verify that these are a precise reproduction of the diffusion process, the root mean square of the distance from the Z-axis $< r^2 >$ is calculated using the simulation results shown in Fig. 7. The root mean square is found to increase in proportion to time t. This proportionate increase is characteristic of the diffusion process, thereby demonstrating that the simulation is a precise reproduction of the diffusion process. These calculations allow us to confirm that simulating particle motion tracking in a turbulent magnetic field can reproduce the diffusion process.

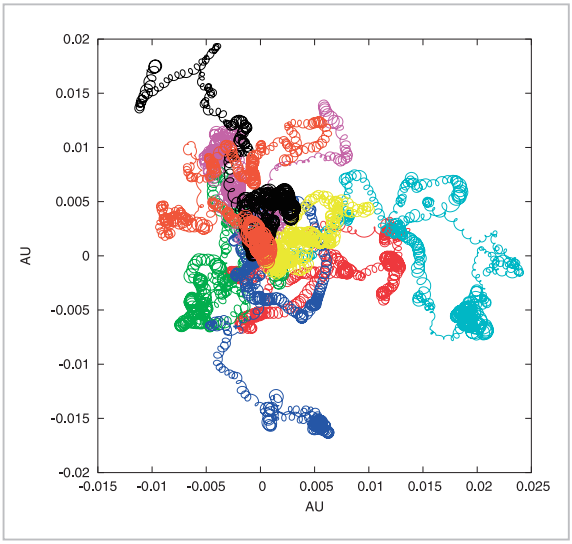

Fig.6 *Simulated motion of 10-MeV particles in a turbulent magnetic field*

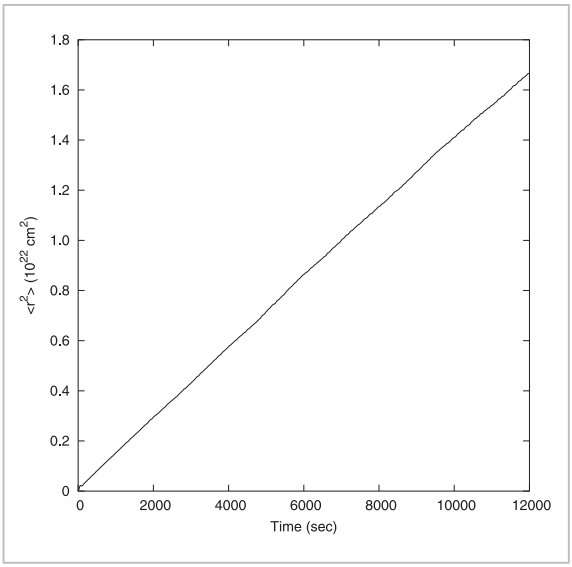

Fig.7 *Time variations in <r²>, root mean square of the distance from the origin calculated from 20,000 simulated particles*

3.2 Propagation of solar energetic particles

We can simulate the process of solar energetic particle propagation through the solar wind by using the method described in preceding section. The solar wind magnetic field is a superposition of the Parker field with a turbulent magnetic field, and the simulation reproduces the propagation of solar energetic particles accelerated near the sun. The effect of a current sheet on the propagation of solar energetic particles is examined below. A current sheet is a structure in which the direction of the magnetic field is reversed on both sides of an extremely thin layer.

Figure 8 plots the positions of simulated 10-MeV solar energetic particles having been reverted toward the sun along the Parker field after arriving at the earth's orbit. This reverting of particles toward the sun along the Parker field makes it possible to cancel out changes in their latitude and longitude resulting from motion in parallel with the magnetic field lines. Hence, the diagram only shows changes in the latitude and longitude of particles resulting from their motion traversing the Parker field, without and with a current sheet (black line) as shown in the left and right panels, respectively. Since the particles are injected at the position of 0 degrees heliographic latitude and -1 degrees heliographic longitude in the solar disk, the particles should be concentrated in the vicinity of location (0, -1) in

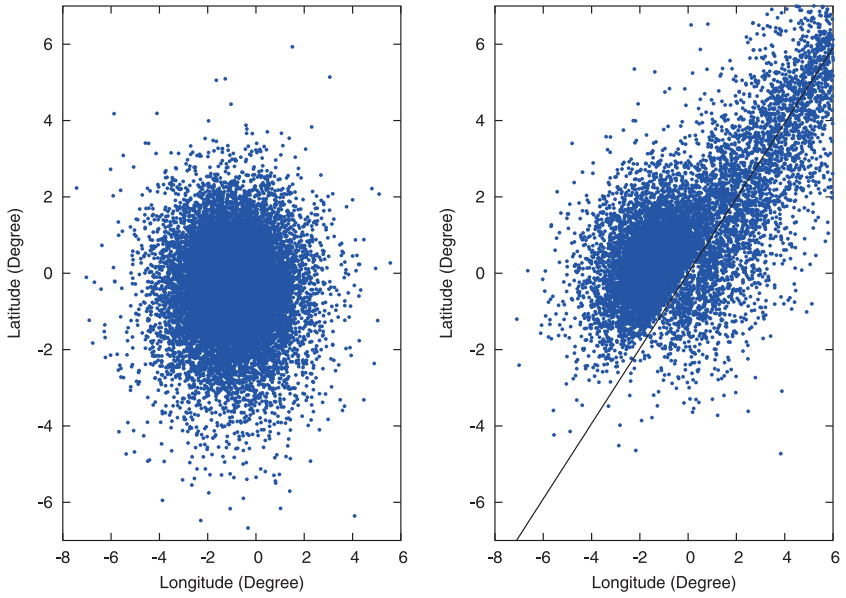

Fig.8 *Positions of particles being reverted toward the sun along the Parker field after arrival at the earth's orbit*

the diagram were it not for a turbulent magnetic field, but both latitudinal and longitudinal distributions are evident in the diagram. This is suggestive of the motion of particles in the direction in which they traverse the magnetic field under the influence of a turbulent magnetic field or current sheet. Without a current sheet, the particles may spread 12 to 13 degrees by diffusion caused by a turbulent magnetic field. Conversely, where a current sheet exists, the travel of particles on both sides of the current sheet would result in drift motion, causing the particles to evidently move along the current sheet. The results of this simulation suggest that, if an active region exists near a current sheet, solar energetic particles accelerated near the sun may be observed even from an observation point (such as the earth) not linked to the active region by a magnetic field line. This might explain the events whereby solar energetic particles accelerated by a flare occurring on the eastern side of the solar disk are observed near the earth.

Figure 9 shows time variations in the particle flux on the earth as calculated from the simulation results, without and with a current sheet as shown in left and right panels, respectively. Of the five lines appearing in each panel of the diagram, the one marked "+0 deg." points to variations observed where, upon the occurrence of a flare, the flare region (particle injection point) is connected to the earth by a magnetic field line; the line marked "−1 deg." points to variations observed where the magnetic field line connected to the earth upon the occurrence of a flare is located 1 degree east of the flare region. Likewise, the lines marked "+1," "+2" and "+3 deg." designate variations observed with magnetic field lines located 1, 2 and 3 degrees to the west, respectively. For the sake of better recognition, each line is offset 0.01 in the y-axis direction. In both panels, the flux rises fast in case of +0 deg., but slower as the earth moves away from the flare region. The flux is somewhat smaller in the presence of a current sheet. Figure 10 also shows time variations in the particle flux on the earth as calculated from the simulation results. The blue line in the diagram marks time variations in the flux on the earth's orbit as observed when the earth

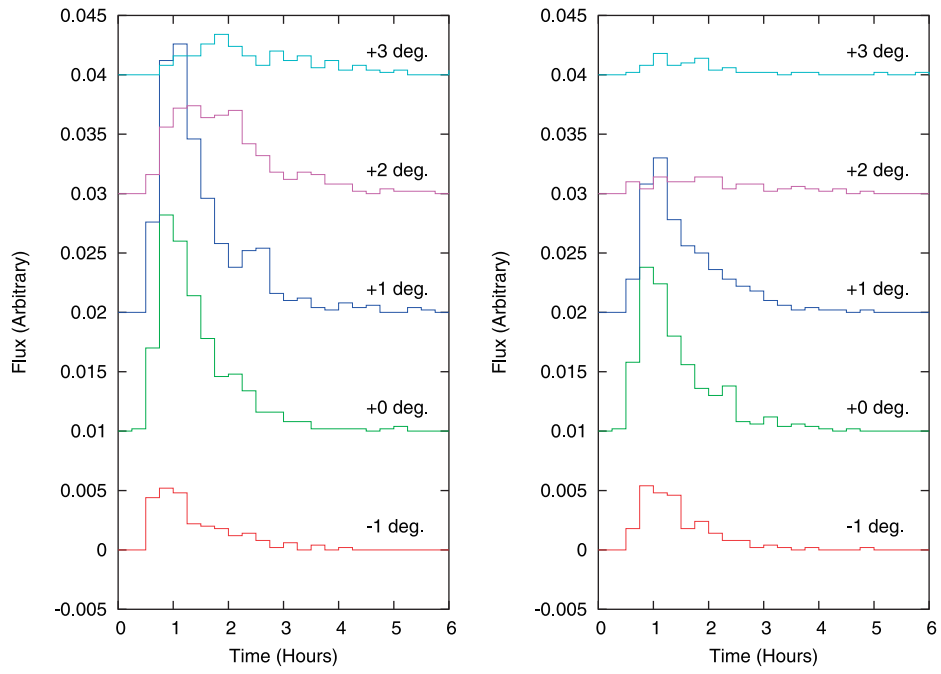

Fig.9 *Time variations in particle flux on the earth*

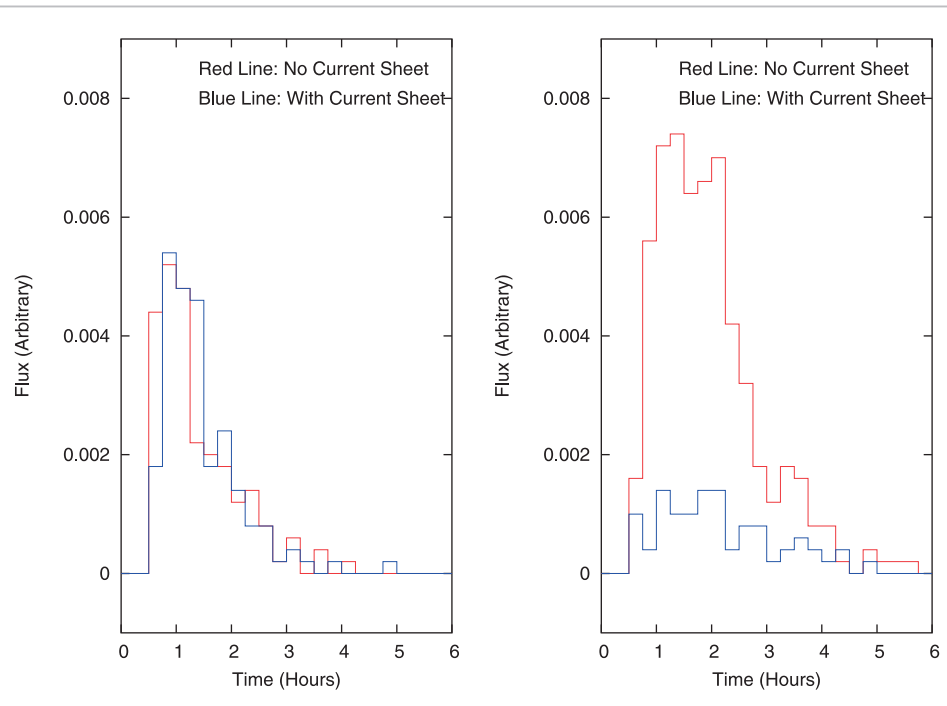

Fig.10 *Time variations in particle flux on the earth*

was located on the same side (left panel) as the flare region with respect to the current sheet, and on the opposite side at the time of flare occurrence (right panel) (see Fig. 11). The red line designates flux in the absence of a current sheet at the same position. Evidently from the left panel of the diagram, the flux exhibits similar variations, regardless of the presence or absence of a current sheet, as long as the flare region and the earth are located on

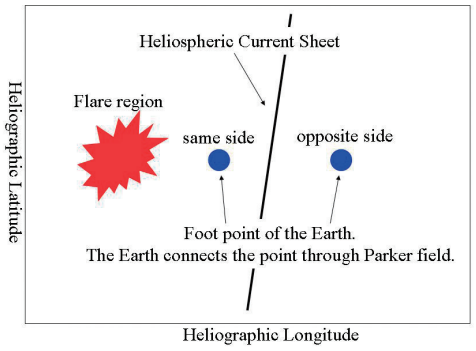

Fig. 11 *Positional relations among flare region, current sheet, and the earth*

the same side. When the earth is located on the side opposite the flare region, however, the time variations of flux exhibit noticeable differences. When the current sheet comes in-between in reference to the right panel, the flux observed from the earth is considerably smaller than that observed in the absence of a current sheet. This is probably due to a diminishing number of particles traversing the current sheet as the particles moved along the current sheet, resulting in less flux.

The presence of various structures, such as a current sheet in the solar wind, could thus have a significant bearing on the process of solar energetic particle propagation and on time variations in the solar energetic particle flux on the earth, thereby stressing the need for a model capable of reproducing solar wind structures in detail for space weather forecasting by means of simulation. Simulations capable of reproducing the structures of solar winds are detailed in References [12] and [13].

4 Space environment event reporting system

One key goal of space weather forecasting is realizing a quantitative forecasting of such space environmental disturbances as solar flares and proton events far in advance of actual occurrence, and then disseminating the relevant information. At the moment, however, much remains yet to be discovered or solved regarding the physical processes of solar flare occurrence and solar energetic particle generation. Moreover, given the few means available for observing the internal conditions of the sun from which these activities originate, we have a very long way to go toward achieving this goal. Perhaps the second best way to disseminate information is collecting observational data in real time in order to spot space environment events sequentially, so that solar flares and increases in solar energetic particles can be identified for immediately reporting events that exceed a warning level as these events occur to alert users.

Since about 10 years ago, information and communications technology has advanced rapidly, shaping up a framework for collecting, processing and reporting various sources of space environment data in quasi real time. As a result, the ability to detect the occurrence of, and changes in, space environment events from observational data in real time and disseminate relevant information promptly has reached a stage of practical usefulness. Real-time dissemination of alarm information should not only help bolster the safety and security of artificial satellite operations, broadcasting and wireless communications, but should also aid in expediting the analysis of failure factors. Moreover, the computer algorithm-based workflow of detecting events and making decisions on whether to report such events is of objective value and, when automated or made autonomous, eases the task of building a scheme of monitoring the space environment around the clock with relative ease. In addition, by setting the address of a cellular phone as a reporting contact address, the owner of the cellular phone can be notified of the occurrence of anomalies by e-mail at any time (provided that the owner is within the cellular phone service area), without resorting to the Internet. For the reasons stated above, we have developed a space environment event reporting system and commissioned it into operation as one of many infor-

mation services.

4.1 System configuration

The system is modularized for each space environment event, such as a solar flare or proton event. Each module consists of an event detection process and an event reporting process. Figure 12 is a schematic diagram of the system configuration. The following explains why each module is divided into an event detection process and an event reporting process.

To understand the properties of space environment events and enhance the technology for predicting the occurrence of such events, it is important to extract and analyze all space environment environments, regardless of scale. The frequency at which space environment events occur, however, is generally known to increase exponentially as the scale of these events narrows. Therefore, if all space environments were reported upon detection, a vast number of notifications-most involving small-scale events-would result. Space environment events that could affect outer space utilization, social infrastructures, etc. are limited to larger-scale events, thereby requiring an additional decision-making process to determine whether to report only those events that have reached a given alert level, in addition to extracting all event information generated. The event extraction algorithm and reporting criteria can also be tuned by editing the parameters coded in the configuration file.

4.1.1 Data flow

NOAA's GOES satellite is equipped with a **S**pace **E**nvironment **M**onitor (SEM) to measure solar X-ray flux, solar energetic particles, and radiation belt particles. Data collected by the SEM is stacked on the SWPC data server in quasi real time. We access this server every five minutes to collect the latest space environment data.

The **A**dvanced **C**omposition **E**xplorer (ACE) satellite is a spacecraft that measures solar wind at the L1 point. ACE supports apparatus designed to measure solar wind plasma (using SWEPAM), magnetic fields (using MAG), solar energetic particles (using EPAM, SIS) and more. ACE is fulfilling an observation mission as part of a global cooperation program to monitor solar winds around the clock. NICT participates in this program to receive data in real time[14]. ACE data is essentially collected in real time as well.

4.1.2 Event detection process

The event detection process is initiated by reading a status file to collect information about the status of the last session of processing (e.g., the extent of processing conducted, whether an event occurred). This information enables the process to determine from when data is processed and in what sequence the detection algorithm is run. There are two basic

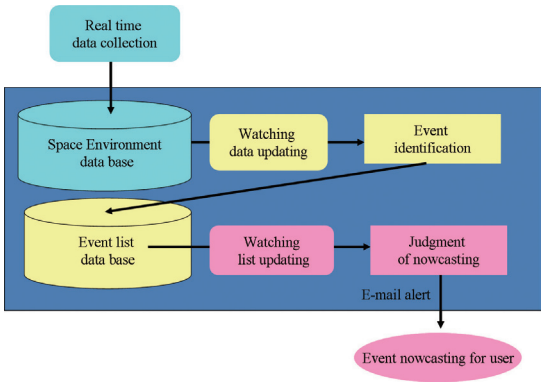

Fig.12 *Space environment reporting system schematic diagram*

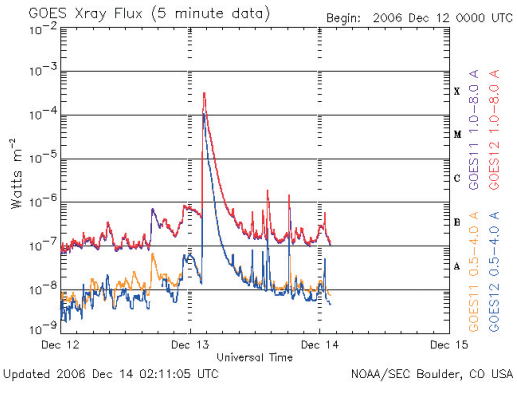

Fig.13 *X3.4 class solar flare observed on December 13, 2006 (reprinted from the SWPC Website)*

methods of event detection as follows:

1) Determine the start of an event using a variation (ΔX) in its physical quantity as a threshold.
2) Determine the start of an event using the size ($|X|$) of its physical quantity as a threshold.

Method 1) is best suited for phenomena involving sharp variations in a physical quantity, such as a solar flare (Fig. 13); method 2) is suitable for gently varying phenomena, such as proton events (Fig. 14). (For more information about the solar flare and proton event detection algorithms, see Appendix.)

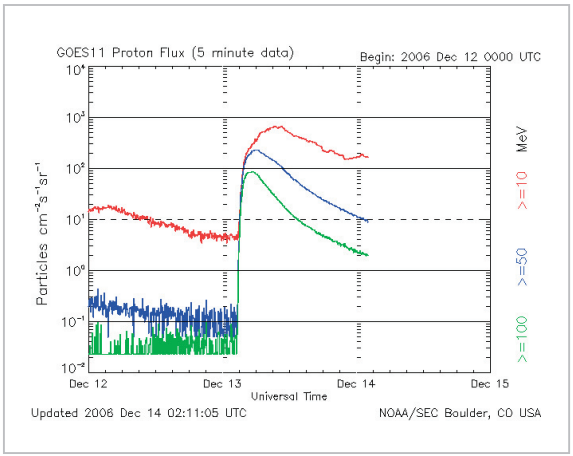

Fig. 14 *Proton event (up to 700 PFU) observed on December 13, 2006 (reprinted from the SWPC Website)*

4.1.3 Event reporting process

Space environment event information extracted by the event detection process is stacked on the server in the form of an event list. By monitoring the updated status of this list to meet a defined reporting requirement, the event reporting process can e-mail event information to registered users as a preliminary report.

Two event reporting requirements are predefined as follows:

1) The scale of an event has reached a specified alert level.
2) The duration of an event has exceeded a specified length.

Requirement 1) is common to all space environment events, whereas requirement 2) applies to long-lasting variations of a proton event or radiation belt particles. Its purpose is alert users to the status of an event now occurring.

The reporting thresholds are described below. This information is coded in the configuration file and can be edited as needed.

[Solar flare preliminary reporting condition]
An M class or higher (10^{-5}Wm^{-2} or higher) flare has occurred.

Table 1 *Solar flare reporting example (for PCs)*

```
Subject: Report of intense X-ray flare
Date: Sun, 03 Jun 2007 11:21:04 +0900
From: main@ml.nict.go.jp
To: ****@**.**.**

2007 年 06 月 03 日 11 時 21 分 JST 通報
GOES-11 衛星の観測から、以下の強い太陽フレアが検出されました。
開始時刻(UT)    強度最大時刻(UT)    終了時刻(UT)    最大強度
  02:06           02:12             02:16           M7.0
提供：情報通信研究機構(NICT) 電磁波計測研究センター

下記のリンク先でイベントのプロットが御覧になれます。
http://mobilep.nict.go.jp/flare-xray/flare-xray_event.php
```

[Proton event preliminary reporting condition]
An event with its 10 MeV or higher proton flux exceeding 10 PFU has started.
A 10 MeV or higher proton flux has exceeded 100,1000,10000 PFU.
A 10 MeV or higher proton flux has fallen below 100,1000,10000 PFU.
A 10 MeV or higher proton flux in excess of 10 PFU has lasted for at least one day.
A 10 MeV or higher variation of the proton event has ended.

Event information is delivered in the format described in Table 1. For the sake of user convenience, the reporting format is available in two versions: one intended for PCs with less text length constraints, and one for portable terminals with a limited displayable text length. In both versions, event-specific information, such as time and physical quantities, is read from an event list into a fixed-phrase template file as variables. For portable terminals, an event graph viewing function is implemented (Figs. 15, 16).

Fig. 15 *Links to the event plot destination (for cellular phones)*

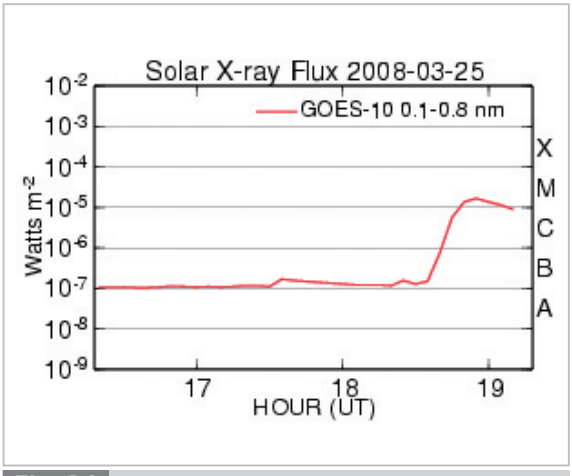

Fig. 16 *Example of event plot (X-ray flare)*

4.2 System operating status

Since its prototype was completed in March 2000, the system has been used as a tool to assist forecasters at NICT. Since February 2004, the system had only been test-run for reporting solar flares and proton events with a view toward verifying its working performance and identifying any problems that might impede steady operation. The test run uncovered delays in e-mail delivery and a need for reporting the start of an event. The system has subsequently gone through modifications and, with an additional repertoire of services being set, has migrated to a production run since April 2005. It now supports a group of just under 700 registered users.

5 Conclusions

This paper discussed the possibilities of a statistical approach and a simulation approach to predicting and issuing alerts on the occurrence of solar energetic particles. Both techniques are still evolving and should benefit from ongoing research. Research on predicting and issuing alerts on solar flares and coronal mass ejections (CMEs), which are the origins of solar energetic particles, is also needed but remains in an evolutionary stage, with statistical probability forecasting being the best method attained thus far[15][16]. As a breakthrough, a space environment event reporting system that automatically detects and issues alerts on the occurrence of solar flares and proton events has been developed. The system provides a useful means of detecting events in the early stages of occurrence and disseminating related information, and has already reached a state of practical usefulness. Thus, research on predicting and issuing alerts on

the occurrence solar energetic particles has been actively pursued from various perspectives and promises a further leap.

Appendix

A.1 Solar flare detection algorithm

The solar flare detection algorithm is described below. Assume that the physical quantity handled (X-ray intensity: Wm^{-2}) and the time series (1-minute value) of timing information are X (t) and T (t), respectively.

1) Checking the status of event detection

Use an event list to check the detection status of a solar flare (no event, event occurring (event start, maximum value)). The subsequent course of processing varies depending on the status of event detection.

2) Detecting "start of event" (1)

If "no event" applies in 1), define the time T (k-3) at which the time-series data at four points [X (k-3), X (k-2), X (k-1), X (k)] initially meets all the following three requirements as a solar flare start time, and assume "start of event" detection:

A) $X(k-3), X(k-2), X(k-1), X(k) > 1.0 \times 10^{-7}$

B) $X(k-3) < X(k-2) < X(k-1) < X(k)$

C) $1.4 \times X(k-3) \leqq X(k)$

3) Detecting "start of event" (2)

If the "start of event" has not been detected in 2), the following algorithm is used to detect "start of event":

Define the time T (k-9) at which the time-series data at 10 points [X (k-9), X (k-8), X (k-7), ...,X (k)] initially meets all of the following three requirements as a solar flare start time, and assume "start of event" detection:

A) $X(k-9), X(k-8), X(k-7), \ldots\ldots, X(k) > 1.0 \times 10^{-7}$

B) $X(k-9) < X(k-8) < X(k-7) < \ldots\ldots < X(k)$

C) $1.2 \times X(k-9) \leqq X(k)$

4) Detecting "maximum value and maximum time"

Detect maximum value X (k) and its time (maximum time) T (k) from the time-series data following "start of event." If the same maximum value spans multiple times, consider the earliest time as the maximum time.

5) Detecting "end of event"

Define the time T (k) at which the time-series data following "start of event" initially meets all of the following two requirements as a solar flare end time, and assume "end of event" detection:

A) $X(k) < (Xstart + Xmax)/2$ (value at "start of event," Xmax: "maximum value")

B) $T(k) > Tmax$ ("maximum time")

The same algorithm as used at the SWPC is used for detecting "start of event" (1). This algorithm, however, is not capable of detecting a moderately starting event, such as a Long-Duration Event (LDE), and therefore has been used in conjunction with the algorithm for detecting "start of event" (2) to detect an LDE.

A.2 Proton event detection algorithm

The proton event detection algorithm is described below. Assume that the physical quantity handled (10 MeV or higher proton flux: PFU) and the time series (5-minute value) of timing information are X (t) and T (t), respectively.

1) Checking the status of event detection

Use an event list to check the detection status (no event, event occurring (event start, rising level, maximum value, falling level)).

2) Detecting "start of event" (rising level 1)

Define the time T (k) at which the time-series data at points num (X (0) to X (num)) initially meets all of the following requirements as an event start time, and assume "start of event" detection:

$X(k) > xlim$

where, xlim = 10

3) Detecting "rising level n"

Define the time T (k) at which the time-series data following "start of event" (including start time) initially meets the following requirement as a rising level n time, and assume "rising level n" detection. This time can even be the start time:

$X(k) > xlv(n)$

where, xlv (2) = 10^2 (level 2), xlv (3) = 10^3 (level 3), xlv (4) = 10^4 (level 4), xlv (5) = 10^5 (level 5)

4) Detecting "maximum value and maximum time"

Detect maximum value X (k) and its time (maximum time) T (k) from the time-series data following "start of event."

5) Detecting "falling level"

Define the time T (k-2) at which the time-series data following the rising level initially meets the following requirement as a falling level time, and assume "falling level" detection:

$X(k-2) < xlv \ \& \ X(k-1) < xlv \ \& \ X(k) < xlv$

[where, $2 < k <$ num]

6) Detecting "end of event"

Define the time T (k-2) at which the time-series data following "start of event" initially meets the following requirement as an event end time, and assume "end of event" detection:

$X(k-2) < xlim \ \& \ X(k-1) < xlim \ \& \ X(k) < xlim$

[where, $2 < k <$ num]

References

1 Fujitaka, K., Fukuda, S., and Yasuda, H., ISBN4–87639–407–5, in Japanese, 2004.

2 Kubo, Y. and Akioka, M., "Existence of thresholds in proton flares and application to solar energetic particle alerts," Space Weather, Vol. 2, S01002, 2004.

3 Garcia, H. A., "Forecasting methods for occurrence and magnitude of proton storms with solar soft X rays," Space Weather, Vol. 2, S02002, 2004a.

4 Garcia, H. A., "Forecasting methods for occurrence and magnitude of proton storms with solar hard X rays," Space Weather, Vol. 2, S06003, 2004b.

5 Posner, A., "Up to 1–hour forecasting of radiation hazards from solar energetic ion events with relativistic electrons," Space Weather, Vol. 5, S05001, 2007.

6 Balch, C. C., "Updated verification of the Space Weather Prediction Center's solar energetic particle prediction model," Space Weather, Vol. 6, S01001, 2008.

7 Laurenza, M., Cliver, E. W., Hewitt, J., Storini, M., Ling, A. G., Balch, C. C., and Kaiser, M. L., "A technique for short-term warning of solar energetic particle events based on flare location, flare size, and evidence of particle escape," Space Weather, Vol. 7, S04008, 2009.

8 Reames, D. V., "Solar energetic particles: Is there time to hide?," Radiat. Meas., Vol. 30, pp. 297, 1999.

9 Zhang, M., Qin, G., and Rassoul, H., "Propagation of Solar Energetic Particles in Three-Dimensional Interplanetary Magnetic Fields," Astrophys. J., Vol. 692, pp. 109, 2009.

10 Dröge, W. and Kartavykh, Y. Y., "Testing Transport Theories with Solar Energetic Particles," Astrophys. J., Vol. 693, pp. 69, 2009.

11 Qin, G., Zhang, M., Dwyer, J. R., and Rassoul, H. K., "Interplanetary Transport Mechanisms of Solar Energetic Particles," Astrophys. J., Vol. 609, pp. 1076, 2004.

12 Nakamizo, A., Tanaka, T., Kubo, Y., Kamei, S., Shimazu, H., and Shinagawa, H., "Development of the 3-D MHD model of the solar corona-solar wind combining system," J. Geophys. Res., Vol. 114, A07109, 2009.

13 Nakamizo, A., Kubo, Y., and Tanaka, T., "A 3–D MHD Simulation Model of the Solar Corona-Solar Wind System," Special Issue of This NICT Journal, 2–3–2, 2009.

14 Maruyama, T., Watanabe, S., Ohtaka, K., and Shimazu, H., "Real Time Solar Wind Monitor Using ACE Satellite," J. Comm. Res. Lab., Vol. 43, No. 2, pp. 285, 1997.

15 Wheatland, M. S., "A statistical solar flare forecast method," Space Weather, Vol. 3, S07003, 2005.

16 Kubo, Y., "Statistical Models for the Solar Flare Interval Distribution in Individual Active Regions," Sol. Phys., Vol. 248, pp. 85, 2008.

KUBO Yûki

Senior Researcher, Space Environment Group, Applied Electromagnetic Research Center

Solar Particle Physics

***NAGATSUMA Tsutomu**, Dr. Sci.*

Research Manager, Space Environment Group, Applied Electromagnetic Research Center

Solar-Terrestrial Physics

***AKIOKA Maki**, Dr. Sci.*

Senior Researcher, Project Promotion Office, New Generation Network Research Center

Solar Physics, Optical System, Space Weather